

*Review Article*

## **Integrating Ice Protection and Noise Abatement Systems for Aircraft Application: A Review**

**Fathima Rehana Munas<sup>1,2</sup>, Yu Kok Hwa<sup>1</sup>, Norwahida Yusoff<sup>1</sup>, Abdul Majeed Muzathik<sup>2</sup> and Mohd Azmi Ismail<sup>1\*</sup>**

<sup>1</sup>*School of Mechanical Engineering, Universiti Sains Malaysia, Engineering Campus, 14300 USM, Nibong Tebal, Penang, Malaysia*

<sup>2</sup>*Department of Mechanical Engineering, Faculty of Engineering, South Eastern University of Sri Lanka, 32360 Oluvil, Eastern Province, Sri Lanka*

### **ABSTRACT**

Aircraft icing remains a key aviation hazard as the global fleet of aircraft in various sectors continues to expand, posing a serious threat to flight safety. As previously stated, the growth of this type of aircraft has been accompanied by an increase in noise levels, and aircraft is reportedly the second most bothersome noise source after traffic. However, integrating an acoustic liner with anti-icing techniques on the leading edge of a nacelle would not efficiently eliminate forward radiated noise and improve the thermal performance of the anti-icing system. Hence, it is of the utmost importance to research the integration of ice protection and noise abatement systems for aircraft applications. This review discusses the integration of ice accretion and noise abatement systems in aircraft applications. The prominence of this review is to explain significant features such as ice protection systems, Computational Fluid Dynamics in ice protection, noise abatement systems, and the integration of ice protection systems and noise abatement systems wherever they are described.

#### ARTICLE INFO

*Article history:*

Received: 06 September 2022

Accepted: 12 April 2023

Published: 08 September 2023

DOI: <https://doi.org/10.47836/pjst.31.6.02>

*E-mail addresses:*

rehana@seu.ac.lk (Fathima Rehana Munas)

yukokhwa@usm.my (Yu Kok Hwa)

menorwahida@usm.my (Norwahida Yusoff)

muzathik64@seu.ac.lk (Abdul Majeed Muzathik)

azmi\_meche@usm.my (Mohd Azmi Ismail)

\* Corresponding author

*Keywords:* Acoustic liner, bias acoustic liner, ice protection, noise abatement

### **INTRODUCTION**

As the global fleet of aircraft in many sectors continues to expand, aircraft icing remains a major aviation hazard that significantly impacts flight safety. Aircraft icing is

characterized by the accretion of ice on aircraft surfaces. Icing occurs frequently on the leading edges of an aircraft's wing, tails, engine inlet, windshield, and helicopter blade (Sreedharan et al., 2014). Moreover, ice accumulation on the rotating spinner positioned at the engine's front surface would impair the uniformity of the inlet flow field, resulting in airflow separation and compressor surge (Zheng et al., 2019). Additionally, ice of the inlet lip would affect the vanes, resulting in mechanical damage and a drop in downstream performance (Shen et al., 2013). The icing on the other surface, i.e., the windshield, would affect output performance and result in energy loss (Yang et al., 2022).

Also, the accumulation of ice on the aircraft tail would impair the stability and control of the aircraft. This phenomenon is most noticeable during landing, cruising, and rising (Ronaudo et al., 1991). Ice buildup on the aircraft wing surface would exacerbate the aircraft's control and stability. Furthermore, the lift force is reduced due to ice on the wing, thus increasing drag and altering moment characteristics (Ronaudo et al., 1991). As a result, the aircraft's fuel consumption increases, thus raising operational costs. Overall, aircraft icing would hinder aircraft performance, increase aircraft weight and drag force, reduce lift forces, and degrade thrust handling, thus creating significant safety concerns (Hassaani et al., 2020).

Therefore, it is necessary to remove ice from aircraft to ensure its safe performance and operation (Shen et al., 2013). As a consequence, several techniques to eliminate ice accretion have been developed. Anti-icing and de-icing are the two primary methods of an ice protection system. The de-icing method removes ice periodically when it has accumulated to a significant thickness (Nagappan, 2013). Electro Magnetic Expulsion and the Pneumatic Inflatable Boot are ice protection devices that use de-icing. On the other hand, the anti-icing method is a prompting system that is activated prior to the onset of icing conditions (Nagappan, 2013). Thermal and chemical fluids are examples of ice protection systems that employ anti-icing methods. Thermal anti-icing is the more prevalent of the two and is classified as either an electric heater or hot bleed air. As previously discussed, an increase in the number of flights is frequently accompanied by a rise in noise levels. It is considered that aircraft noise is the second most infuriating source of noise after traffic noise (Ives, 2009). Researchers have proposed several solutions for reducing engine and turbine noise, including installing an acoustic liner (AL) in a noise cowl zone. However, combining an acoustic liner and anti-icing on the leading edge of a nacelle lip skin would not be adequate to boost thermal performance (Ismail, 2013). Therefore, it is of the utmost importance to research the integration of ice protection and noise abatement systems for aviation applications.

This review discusses the integration of ice protection and noise abatement systems in aircraft applications, particularly focusing on ice protection systems, CFD in ice protection, and noise abatement systems.

## ICE PROTECTION SYSTEMS

Ice protection has been an important component of all aviation for a long time. The United States National Transportation Safety Board (2007) reported that icing problems caused many aircraft crashes. Chemical fluid, mechanical, thermal, hybrid, and other ice protection methods are widely used in commercial aircraft. The chemical fluid ice protection method removes ice deposits and forms a protective film on airplane surfaces (Grishaev et al., 2021). This method protects aircraft surfaces from icing by lowering the freezing temperature of supercooled water below the ambient temperature by mixing a chemical fluid with supercooled water that has been impinged. The mechanical ice protection method, i.e., pneumatic inflatable boot, on the other hand, breaks the ice's bond from the aircraft's surface, and the ice fragments are blown away into the atmosphere. Also, the thermal ice protection method uses hot bleed air or electricity to the protected aircraft surface. Lastly, a hybrid ice protection system comprises a running wet electro-thermal anti-icing system and an Electro-Mechanical Expulsion De-icing System (EMEDS). While the former system maintains temperatures above freezing point, the actuators of the latter system periodically eradicate ice.

Two systems in aircraft ice protection are widely used in commercial aircraft: the anti-icing system (AI) and the de-icing system (DI). The DI system removes or breaks ice accumulation periodically, while the AI system prevents ice from always forming on aircraft components. Therefore, it is understood that the fundamentals of ice protection tools can guide researchers in recommending the most appropriate ice protection device for a given icing condition. The types of ice protection tools are described, and their strengths and weaknesses are listed in Table 1.

Table 1  
*Types of ice protection devices*

Examples of Ice Protection Devices	AI/ DI	Strengths	Weaknesses
Mechanical Deformation Ice Protection	DI	These are light and have low operational costs. Useful for small aircraft. Less energy consumption and maintenance and the cost and weight are comparably small and reliable (Li, 2012).	Special compound material and stretchable fabric-reinforced elastomer are needed for PIB to avoid weathering and erosion.
Electro-Mechanical Expulsion Ice Protection System	DI	Mostly used to lift aircraft surfaces, such as wings. Low power consumption. The cycling time would be controlled and varied. Efficient and automatic ice protection	Conductive strips should be fabricated on the flexible dielectric sheet.
The Pulse Electro-Thermal Ice Protection Systems (PETD)	DI	Low energy consumption is required. Very useful on the windshields of many modes of transportation, including airplanes, bridges, and automobiles. (Petrenko, 2005).	Difficult to manage ice formation outside the ice protection area (Ma, 2011)

Table 1 (continue)

Examples of Ice Protection Devices	AI/DI	Strengths	Weaknesses
Thermo-Mechanical Expulsion Ice Protection System	AI	This system provides excellent anti-icing performance while consuming less energy (June 2020).	This system is too expensive (Jun et al., 2020).
Thermal Ice Protection System	AI	The optimum heat transfer from the jet to the impinging surface occurs at a distance from the hole to the impinging surface of 5-7 times that of the jet diameter (Raghunathan et al., 2006).	Weight and manufacturing costs are comparatively high (Syed et al., 2018). Higher energy costs are required.
Hybrid Ice Protection System	DI and AI	It is a more cost-effective method instead of using hot air.	Warm and high liquid water content condition is required.
Double-walled Ice Protection System	AI	Provides a more uniform temperature. Avoids hotspots occurring on the nacelle lip skin.	Disrupts installation of noise abatement material. Complex construction is required, resulting in higher installation and maintenance costs (Birbragher, 1988).
Chemical Liquids Ice Protection System	DI and AI	Useful in small aircraft	The required glycol solution must be carried on board. Limited duration of ice protection (Ramamurthy et al., 1991).
Swirl Ice Protection System	AI	Construction is very simple in comparison to other ice protection systems. Provide uniform temperature distribution on the nacelle lip-skin, preventing the runback ice accretion on the downstream area.	A huge amount of hot air is required.

### Mechanical Deformation Ice Protection

The pneumatic inflatable boot (PIB) is a mechanical deformation ice protection device commonly used in light airplanes. The development of the inflatable boot began in 1928, and this has been used in more than 30,000 small aircraft worldwide (Ramamurthy et al., 1991). This device has inflatable rubber strips on the wings' outer surface and control surfaces where ice is accreted (Ronaudo et al., 1991). The ducts inside the rubber strips function as an air conduit and become inflated when they receive pumped air from the engine. Due to the combination of shear, bending, and peel forces, the surface distorts and breaks the ice down. Then the broken ice is carried away from the surface by aerodynamic force (Ramamurthy et al., 1991). The working principle of the pneumatic inflatable boot is shown in Figure 1.

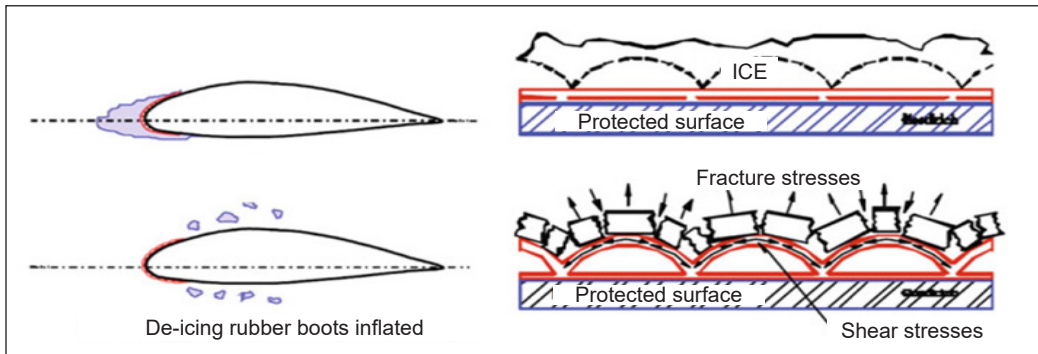


Figure 1. Working principle of Pneumatic Inflatable Boot (PIB) (Battisti, 2015)

### Electro Impulse Ice Protection System

This system ensures the aircraft's safety during icing conditions. The capacitors are discharged through an electric coil. This system produces a huge magnetic field and, thus, large amplitude and impulse, which act on a nearby electrically conductive plate. The impulse force exerted on the nacelle's surface slightly expands, then contracts, generating mechanical vibrations on the leading edge. As a result, ice on the surface is shed due to mechanical vibration caused by the Electro Impulse Ice Protection System's impulse forces (Li, 2012). Figure 2 shows the elementary circuit of this ice protection system. In this system, the pulse coils are connected to a high voltage capacitor by low resistance, low inductance cables. When the switch is turned on, the discharge of the capacitor through the impulse coils creates a rapidly forming and collapsing electromagnetic field. According to Maxwell's law, it is known that the time-dependent magnetic field induces eddy currents in the metal skin. Therefore, the Lorentz force formula obtains the instantaneous impulse force of several hundred pounds in magnitude. However, the duration is only a few hundred microseconds. A small amplitude, high acceleration movement of the skin acts to shatter, de-bond, and expel the ice (Jiang & Wang, 2019).

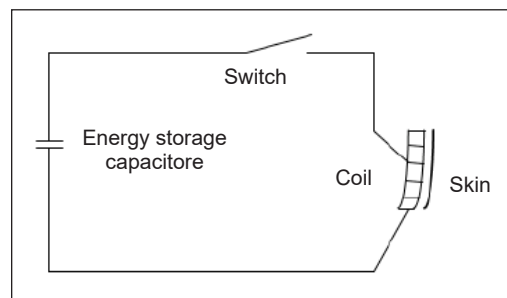


Figure 2. Working principle of Electro Impulse Ice Protection (Jiang & Wang, 2019)

Therefore, the Lorentz force formula obtains the instantaneous impulse force of several hundred pounds in magnitude. However, the duration is only a few hundred microseconds. A small amplitude, high acceleration movement of the skin acts to shatter, de-bond, and expel the ice (Jiang & Wang, 2019).

### Electro-mechanical Expulsion Ice Protection System

This system is a modern ice protection technique used in aircraft. In this case, opposing electromagnetic fields are generated in actuators by a high-current electric pulse, which causes the actuators to deflect. This deflection is then transmitted to the erosion shield, which bends and vibrates at a very high frequency. As a result, the accumulated ice on

the erosion shield is released (Goraj, 2004). The working principle of this type of ice protection system is shown in Figure 3.

### The Pulse Electro-thermal Ice Protection Systems (PETD)

It is an improvement of the Electro-Thermal Ice protection system that uses an electro-thermal pulse approach. This system encompasses strips and shedding zones as heating components. While the partition strips maintain the surface temperature above freezing, the shedding zones melt the ice contact on the leading-edge surface (Ma, 2011). In addition, the thin ice layer is melted by high-density power, which reduces the amount of melted runback water. Figure 4 displays the working principle of this type of system. In this system, the airflow cools the skin temperature below freezing very quickly when the power is cut off. Thus, the impinged water freezes quickly, resulting in minimal runback ice formation.

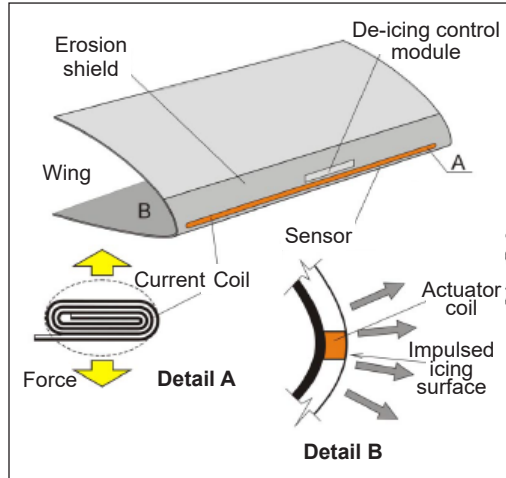


Figure 3. Working principle of Electro-Mechanical Expulsion Ice Protection System (Goraj, 2004)

### Thermo-mechanical Expulsion Ice Protection System

It is a hybrid system designed to provide ice protection on icing surfaces using less power. This system employs a resistive heater connected to the leading edge, with special attention paid to the impingement zone where the incoming air stream divides between upper and lower surfaces and engineering applications require additional time (Al-Khalid, 2007). Figure 5 shows a schematic representation of the system.

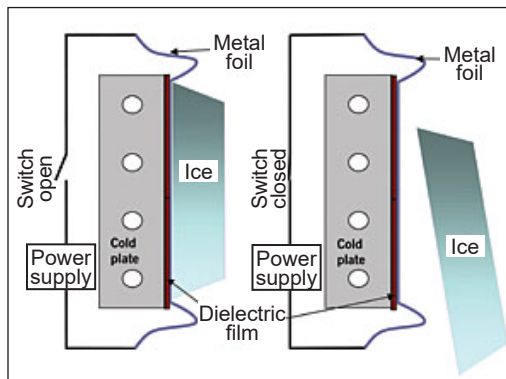


Figure 4. Working principle of PETDS (Pulse Electro Thermal De-icing, 2005)

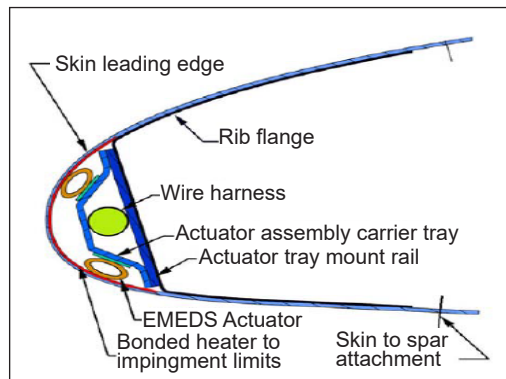


Figure 5. Thermo Mechanical Expulsion Ice protection system (Al-Khalid, 2007)

### Thermal Ice Protection System

In this technique, thermal energy is transferred to the nacelle lip skin as well as a wing in modern commercial aviation (Khai et al., 2020). This energy evaporates the impinging water, a consequence of keeping the surface temperature above freezing. Particularly, Piccolo Tube Anti Icing (PTAI) is one of the most popular thermal anti-icing systems for aircraft, and it has staggered holes around the tube. The engine compressors supply hot air at high temperatures and pressure. This hot, high-pressure air is then introduced to PTAI, where the supply pipe is directed toward the internal surface through discrete holes in the perforated piccolo tube. After impinging on the internal surface, the exhaust air circulates the D-chamber and exits through the exhaust grill, as shown in Figure 6 (Ismail, 2013). In this case, the pneumatically operated valves control the PTAI system. The hot air is distributed via a piccolo tube that runs the length of an aircraft slat within the D-chamber (Raghunathan et al., 2006).

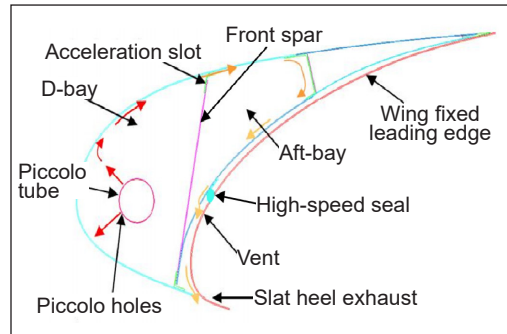


Figure 6. Thermal Ice Protection System (Ismail, 2013)

### Hybrid Ice Protection System

The fundamental concept of this system is similar to that of the Thermomechanical Expulsion Ice protection system. Electric heaters and a low-power ice protection system are combined to reduce energy consumption, which is therefore known as a hybrid anti-icing system (Al-Khalil et al., 1997).

### Double-walled Ice Protection System

It is another alternative ice protection system, as shown in Figure 7. This system forces hot air from the D-chamber into a channel between two walls. Consequently, the heat from the hot air is transferred to the walls by convection (Rosenthal & Nelepovitz, 1985). This method provides a more uniform temperature distribution and prevents the occurrence of hotspots on the nacelle lip skin.

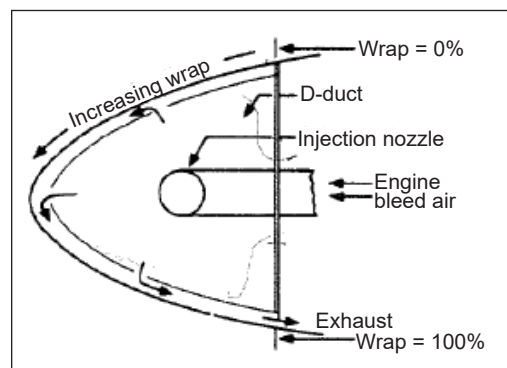


Figure 7. Doubled-walled Ice Protection System (Rosenthal & Nelepovitz, 1985)



## Chemical Liquids Ice Protection System

The chemical ice protection system works by lowering the freezing point of an ethylene glycol-based fluid through laser-drilled titanium panels on the leading edges of the wings, horizontal and vertical stabilizers, and a slinger ring that protects the propeller. The fluid is dispersed as air flows over the wing and empennage, coating the surfaces and preventing the formation and adhesion of ice (Whitfeld, 2021).

## Swirl Ice Protection System

This system transfers high-pressure and high-temperature air from the jet engine to the D-chamber by a supply pipe (Ismail & Wang, 2018). The nozzle is located at the end of the supply pipe and bent 90° to direct the high-pressure, hot air into the D-chamber. The air with a high temperature and velocity exits the nozzle and comes into contact with the cooler air in the D-chamber, causing a relatively large amount of cold air to be entrained by hot air. Thus, the air is entrained in a circular motion around the annular D-chamber. As a result, this system transfers heat from hot air to the nacelle lip skin more uniformly than other ice protection systems (Ismail, 2013).

This technique has a variety of nozzle designs and arrangements which enhance heat transfer and temperature distribution in stationary air due to turbulent enhancement, thus increasing the mixing process between hot air and stationary air. As a result, the duration of heat and momentum transfers from hot air to the nacelle lip skin has been reduced significantly (Syed et al., 2018). Figure 8 illustrates a schematic representation of this type of system.

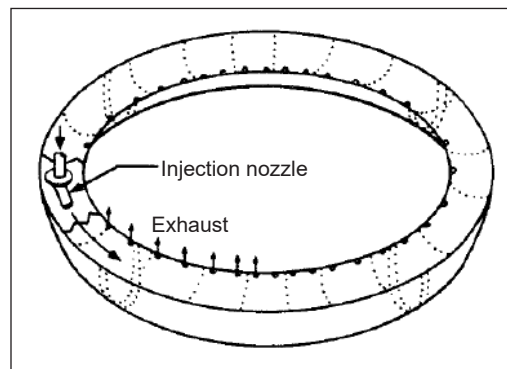


Figure 8. Swirl Ice Protection system (Rosenthal & Nelepovitz, 1985)

## CFD APPLICATION IN ICE PROTECTION SYSTEM

Many researchers use CFD applications in anti-icing due to the difficulty and cost constrain in experiments and validation tests. Previous researchers applied CFD techniques to optimize the performance of hot-air anti-icing systems, particularly Piccolo Tube Anti Icing (PTAI). Al-Khalil et al. (1997) investigated the performance of hot-air anti-icing using engine inlet ice protection. Here, the authors utilized trajectory code to estimate local water-impingement rates on the nacelle inlet surface. The temperature distribution on the nacelle lip skin was determined by solving the energy balance on surface runback water and nacelle lip skin. According to the results, the authors recommended that a large amount of heat be concentrated on the stagnation point of water droplet impingement



to evaporate these water droplets. The results also showed that the runback water might reach freezing temperature downstream of the nacelle lip-skin. Therefore, the authors also suggested protecting this area with moderate thermal anti-icing systems, such as Electro Thermal Heaters (ETH).

Subsequently, Morency et al. (1997) introduced a simple mathematical model to analyze the heat transfer phenomenon on the aerofoil surface. This mathematical model was used to simulate the temperature changes of the runback water film and the conduction in the airfoil's skin. The results demonstrated that evaporation heat loss increases with temperature more rapidly than convection heat loss.

Later, Smith and Taylor. (1997) examined the simulation of a 2D anti-icing system in dry and wet conditions using the PHEONICS code. This code solved the energy equation to determine the cooling effects of water impingement. The simulation result was congruent with the flight test. Afterward, Croce et al. (1998) obtained the predicted results from the FENSAPICE code they had developed. The code utilized a finite element method to determine ice accretion, droplet impingement, and conjugate heat transfer by solving the Navier-Stokes equation. They used a standard k-epsilon model to resolve turbulent flows inside the wing's leading edge. Their results were claimed to be satisfactory. However, there was no validation against experimental results. In addition, de Mattos and Olivera (2000) studied conjugate heat transfer on an anti-icing system wing slat using the FLUENT CFD code. The results showed that the heat transfer characteristics were proportional to the mass flow rate of hot air.

Morency et al. (2000) once again developed a numerical code and implemented it into a CANICE CFD code to design an ice protection system on wing-leading edges. The boundary layer equations were solved by the finite difference method and integral method. The results showed that the finite difference method was able to give results that were in good agreement with experimental results obtained by the integral method. Hua and Liu (2005) used the FLUENT CFD code to predict the temperature distribution along the wing's leading edge. They focused on two-dimensional bay slice approximations to obtain predicted results. This method needed a low number of meshes and the shortest time for the convergent. Further, the authors compared the results from the flow field of the two-dimensional bay slice with those from the flow field of the three-dimensional simulation. The comparison concluded that the results of the two-dimensional bay slice had overestimated the vortex area inside the wing leading edge and the wing leading edge temperature, confirmed by experimental results.

Subsequently, Planquart et al. (2005) employed the FLUENT CFD code to map heat transfer coefficients in a multi-impinging jet anti-icing system. The authors observed that their simulation results were relatively close to the experimental data for the surface heat transfer coefficients measured by infrared thermography. Rigby (2006) later conducted a

numerical analysis of the diamond hole arrangement of PTAI. He utilized a GLENNHT code, which employed a standard k-epsilon model to fix the turbulent flow of jet impingement, to forecast anti-icing performance. The author presented that a significant improvement occurred even if a small amount of total heat was supplied to PTAI in the design.

Papadakis and Wong (2006) then applied the FLUENT CFD code to examine the effect of piccolo tube configuration on the temperature distribution of the wing leading edge. They reported that the predicted results closely matched the experimental results they obtained in the same study. According to their investigation, the best configuration of the piccolo tube occurred when the piccolo pipe center was 0.75 inches and 0.193 inches behind and under the wing highlight, respectively.

Hua et al. (2007) developed 3D unsteady thermodynamic models to characterize the dynamic response of an aircraft wing anti-icing operation. The results obtained by the authors demonstrated that the three-dimensional CFD unsteady simulation yielded an outstanding correlation with the flight test. However, the 2D unsteady simulation underestimated the increment of skin temperature at the initial period and suddenly overestimated the increment of skin surface when the flow was well set up.

Wang et al. (2007) used the FENSAPICE CFD code to investigate PTAI performance on the wing slat under wet conditions. Based on the findings, they recommended double-wall anti-icing on the lower slat surface to prevent icing on the wing leading edge surface. In the same year, Elangovan and Hung (2007) formulated a new C++ code to predict the temperature distribution on the wing leading edge, the minimum heat required for PTAI, and skin temperature. A comprehensive experimental and numerical study of PTAI was conducted by Wong et al. (2009). The authors predicted the temperature distribution on the leading edge of a wing in wet and dry conditions using the FLUENT CFD code. In this method, the authors could determine the minimum heat requirement of PTAI to protect the wing from icing. The skin temperature prediction has been achieved by using alternating direction implicit methods. The proposed heat transfer correlations and their applications have been published in heat transfer literature to estimate heat transfer of impinging jets on the inside skin. They also utilized thermodynamic energy transfer rate to resolve thermodynamic energy and boundary conditions on the external wing skin. The simulation showed that the wing skin temperature under dry conditions was higher than that under wet conditions.

Domingos et al. (2010) then developed a 2D computational method to analyze hot-air anti-icing systems. Using this method, they could predict the temperature of the wing leading edge in both dry and wet situations, as well as the runback ice phenomenon. Reid et al. (2012) conducted a numerical simulation of in-flight electro-thermal anti-icing using a conjugate heat transfer technique, which had been implemented in FENSAPICE for solving complex heat transfer phenomena. Here, the external and internal flow was

decoupled before being used to provide boundary conditions to the steady-state thermal dynamic model. They used a 2D RANS equation with SST  $k-\omega$  turbulent model to compute gaseous phase flow for external flow. A Nusselt number correlation was also used to solve the heat transfer problem in the internal flow module. It is claimed that the simulation results showed good agreement with experimental data for both dry and wet conditions.

Following that, Bu et al. (2012) proposed mathematical models and a numerical code for the simulation of thermal ice protection. In their study, heat transfer coefficient distributions were determined using the boundary layer integral method, and the external flow field and local water collecting efficiency statistics were predicted with the Eulerian method. This numerical code also calculates airfoil equilibrium surface temperature, the mass flux of runback water, and runback ice mass flux. In addition, a user interface is developed to integrate the computation fluid dynamic code to achieve a method for analyzing a thermal anti-icing system.

A fully three-dimensional ice accretion model was developed by Shen et al. (2013) to characterize ice shapes at the engine inlet. They determined the film flow direction and the mass flux distribution of the runback water using the shear stress on the inlet surface. Hannat and Morency (2014) introduced an anti-icing conjugate heat transfer method based on the ANSYS-CFX flow solver and FENSAP-ICE software. Later, Bu et al. (2013) analyzed the performance of the hot air ice protection system to calculate the external heat transfer coefficient and thermal conductivity. Sreedharan et al. (2014) generated a CAD model of the wing-piccolo tube using CATIA software. The discretization of the flow domain and the steady-state CFD analysis of the internal and external flow field were performed using ANSYS ICEM CFD and the ANSYS FLUENT, respectively. It was observed that a piccolo tube-wing surface spacing of 9 mm provides desired temperature distribution. Ismail and Abdullah (2015) then investigated the factor influencing the temperature distribution on the nacelle lip. They demonstrated that the temperature deviation coefficient increases as the nozzle diameter increases while the nacelle lip skin average temperature drops as the average air velocity inside the nacelle lip decreases. However, the authors have not studied the temperature distribution on the nacelle lip with bias flow.

Cao et al. (2016) presented a numerical simulation of three-dimensional ice accretion on an aircraft wing. In this study, they derived the governing equations for supercooled droplets in three-dimensional applications using the conservation of mass and momentum laws. The droplet phase was regarded as pseudo-fluid. Furthermore, some meteorological parameters involved in ice accumulation were also investigated in this study. In a separate study, a 2D simulation of thermal Pitot tube de-icing was conducted by Asante et al. (2016). By applying heat to the walls of the pitot probe, they determined the time taken to melt the ice surrounding the pitot probe. Azam et al. (2016) subsequently investigated the effect of

bias flow on the lift and drag forces. With a bias acoustic liner, the drag coefficient of the nacelle lip is reduced by 90.5% compared to without a bias acoustic liner.

Zhou et al. (2017) published an article on temperature and runback ice prediction methods for three-dimensional hot-air anti-icing systems. According to their findings, two parameters, such as liquid water content and Mach number, significantly affect runback ice accretion. Syed et al. (2018) used one-way fluid-structure interaction (FSI) to investigate the influence of the Reynolds number based on the effective impingement surface of the piccolo tube anti-icing system on the maximum thermal stress and strain of the nacelle lip skin for different aluminum series. According to their simulation, the maximum strain increases with the Reynolds number. The maximum stress, on the other hand, rises to a peak and then quickly decays with the Reynolds number.

Liu et al. (2019) proposed a three-dimensional ice accretion model to simulate a stratospheric airship icing performance in an ascending process. Rohini et al. (2019) conducted additional research to compare the performance of a rotating piccolo tube with a piccolo tube using CFD. Based on the results, the piccolo tube model performed better in temperature distribution and had a higher surface temperature than the rotational piccolo tube model. However, a higher and more concentrated temperature zone was obtained for the fixed piccolo tube model.

The effect of ice accretion on an aircraft's longitudinal aerodynamic properties was then investigated by Cao et al. (2020). An engineering prediction of the longitudinal aerodynamic derivatives was established based on the individual component CFD calculation and narrow strip theory. Based on the flight test data, the longitudinal aerodynamic parameters of clean aircraft and icing aircraft were calculated. Based on their findings, the icing makes an aircraft's lift and elevator less effective, and increases drag. Barzanouni et al. (2020) numerically investigated the blowing-out impact on the NACA0012 airfoil surface to prevent ice accretion. The shear-stress transport  $k-\omega$  model was selected to simulate the turbulence closure model and make better predictions. The results demonstrated that the diameter and pitch of the holes are important parameters for reducing ice accretion and ice weight, respectively.

Khalil et al. (2020) examined the effects of hot air arrangement from a piccolo tube using ANSYS software. In their studies, three distinct jet configurations were used: an inclined shape with one jet row, a staggered shape with two jet rows, and a shape with three jet rows. Based on the results, the third shape covers a larger surface area on the leading edge as compared to the other two shapes.

Following this, Bu et al. (2020) carried out a numerical simulation of an aircraft thermal anti-icing system based on a tight coupling method. The authors have established the heat and mass transfer model of runback water. According to the results, this approach produces downstream surfaces with a greater temperature and a lower drop rate. It contributes to

a higher convective heat transfer coefficient. In another study, Hassaani et al. (2020) performed a numerical investigation of the thermal anti-icing system of the aircraft wing. Three-dimensional Navier-Stokes codes were used to simulate jet flow impinging on aircraft leading edge surfaces, and the numerical results were claimed to be in excellent agreement with the experimental data. In the same year, Huanyu et al. (2020) investigated the optimisation of a simulated icing environment by altering the arrangement of nozzles in atomization equipment for aircraft anti-icing and de-icing. According to the authors, the study's findings will contribute to creating a better-simulated icing environment.

Wang et al. (2022) investigated the numerical simulation of aircraft icing under a local thermal protection state. The authors demonstrated the method for icing by considering the water film flow. They designed different protection ranges and powers and simulated them under different conditions. They found that when the protection range is large, and the protection power is low, the ice will accumulate in the protection range. Further, ice will accumulate outside the protected area when the protection range is small. They also claimed that the ice ridges degrade the aerodynamic characteristics. Bennani et al. (2023) presented the numerical simulation of an electro-thermal ice protection system in AI and DI mode. The authors presented the models to describe the behavior of the thermal protection system and unsteady ice accretion. They used many methods to solve the boundary layer flow, and the solvers were used to compute the heat transfer coefficient. They also claimed that this approach is easier to prolong to a three-dimensional solver than the Prandtl boundary layer solver.

## **NOISE ABATEMENT SYSTEMS**

The concept of noise abatement has been around since the Greek civilization. The ancient Greeks used this concept to absorb and amplify sound, and their acoustic absorption coefficient was at its highest value when fluid trapped inside resonated (Hoffman, 2007). On the other hand, noise abatement tools are installed on commercial aircraft to reduce excessive engine noise that may cause noise pollution in the surrounding environment (Azam & Ismail, 2018). In this sense, porous material has been introduced and incorporated to enhance the acoustic resistance of the acoustic liner. In contrast to the air cavity of the Helmholtz type, as depicted in Figure 9, porous materials are effective acoustic energy absorbers throughout a broad frequency range. Despite being commonly used in air-conditioning and motorcycle exhausts, this material is unsuitable for aircraft applications due to a tendency to migrate, fracture, and blind due to ash, dust, or liquid (Amin & Garris, 1996). As a result, modified acoustic liners for aircraft applications have been introduced, and these types of acoustic liners comprise porous plates, honeycomb channels, composite woven materials for acoustic absorbent, and the backplate sheet, as displayed in Figure 10 (Azam et al., 2017). Bias acoustic liners (BAL) have also been developed to advance this technique.

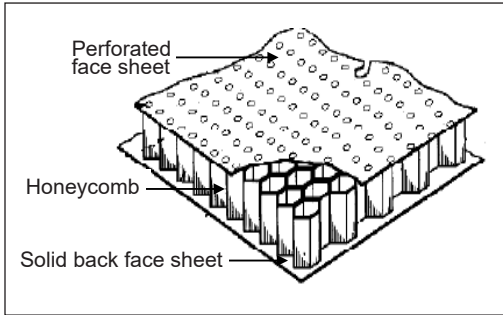


Figure 9. Perforated face system (Moe et al., 2009)

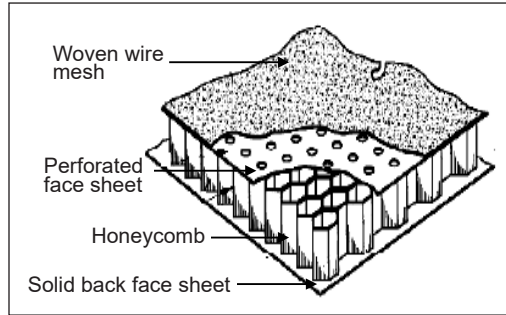


Figure 10. Modified acoustic liners (Amin and Garris, 1996)

### Bias Acoustic Liner (BAL)

With technological advancements, the Boeing Company patented an improved version of an acoustic liner known as the BAL, which uses hot air from the compressor (Ives, 2009). The benefit of using BAL is that it produces bias flow, which has a greater impact on acoustic absorption (Sun et al., 2002). The bias acoustic liner and bias flow within the bias acoustic liner are represented in Figures 11 and 12, respectively.

The performance of BAL for noise reduction is also important. BAL behaves similarly to Helmholtz resonators that allow noise reduction within an optimized frequency range. As a result, BAL is suitable for fan noise, which is essentially atonal noise. Superimposed layers of BAL, known as 2 degrees of freedom or 3 degrees of freedom acoustic liner, are typically used to broaden the absorption range (Leylekian et al., 2014).

Research has been carried out to analyze the noise abatement effect of BAL, although there were just a few. Legendre et al. (2014) investigated sound absorption using an acoustic liner with bias flow. Based on their results, BAL with bias flow at a small Mach number changes the acoustic pressure in the boundary layer, thus improving its acoustic properties. Azam et al. (2017) presented a state-of-the-art noise abatement system in commercial

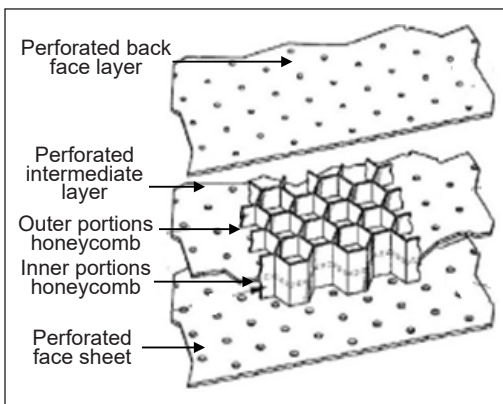


Figure 11. Bias acoustic liner (Breer et al., 2021)

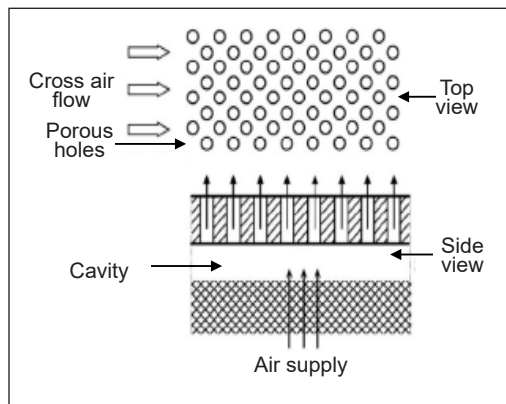


Figure 12. Bias flow diagram (Azam et al., 2016)



aircraft using BAL. According to their article, the BAL has an excellent noise-absorbing capacity and is best used with the nacelle anti-icing system liner on the nacelle lip skin. Azam and Ismail (2018) researched the effect of BAL on the lip skin of the nacelle on civil aircraft and claimed that BAL significantly improves the aerodynamic performance of the nacelle lip skin.

Thanapal et al. (2019) investigated the effect of perforated liners' porosity in the presence of grazing flow. According to their findings, acoustic amplification will occur instead of damping when the perforated liner has very low porosity. Increasing porosity will increase the acoustic damping capability of the perforated liner until optimal porosity is attained. Further increase in porosity will affect the performance of liners. Khai (2021) conducted additional CFD research to study the thermal characteristics of the AL and BAL in real flight conditions. The study concluded that the thermal performance of hot air anti-icing systems with BAL is improved over those with AL and without any noise abatement tools and is directly proportional to the number of BAL.

## **INTEGRATING ICE PROTECTION SYSTEM AND NOISE ABATEMENT SYSTEM**

Integrating ice protection systems with noise abatement systems is vital in aircraft applications to eliminate thermal hotspots as well as noise pollution. In most aircraft anti-icing systems that use hot bleed air, ice can be melted, which can cause the nacelle surface to overheat due to non-uniform temperature distribution. Acoustic liners have been developed to reduce noise while cooling the combustion chamber. However, acoustic liners have desirable acoustic properties for absorbing excessive engine noise. Due to their poor heat transfer characteristics, which lower the overall temperature of the lip skin surface, these have an adverse effect when combined with hot air anti-icing. Consequently, a higher anti-icing temperature must be supplied to hot air in the nacelle D-chamber, thus increasing engine power, consumption, and expense (Khai, 2021).

Several studies have examined the aerothermal properties and noise abatement effect of BAL. Ives (2009) reviewed the current state of the art of aerothermal properties of acoustic liners. Based on their review, the author concluded that the heat transfer rate may be insufficient due to the flow and thermal properties of the acoustic liner. Further studies have been conducted on the noise abatement system in a nacelle lip skin application.

Khai et al. (2020) investigated hot air anti-icing adjoining with a noise abatement system using a bias acoustic liner. The study concluded that the BAL has tunable sound absorption characteristics due to various bias flow velocities through the perforated faceplate. This sound absorption property gives BAL a higher heat transfer rate and a longer lifespan than AL (Ma & Su, 2020).

Researching the integration of the ice protection system with the noise abatement system is crucial. However, only a few studies have been initiated to date. According to



the research by Ives et al. (2011), the heat transfer coefficient of BAL is higher than that of AL as fluid can pass through two porous plates in BAL, whereas only one porous plate exists in AL. As a result, the active area for heat transfer between a fluid and a solid surface in BAL is approximately double that of AL (Ives, 2009).

Studies were performed by Ibrahim et al. (2018) to examine the effect of the perforation shape of a perforated fin during heat transfer. They revealed that the perforation on the fin facilitates heat transfer with higher turbulence intensity. Additionally, the turbulence intensity depends on the shape or geometry of perforations. Since the higher turbulence intensity causes rapid heat dissipation, BAL with a perforated back-face sheet has a higher heat transfer rate than AL.

Therefore, scientists and researchers have proposed incorporating BAL into aircraft anti-icing systems to diminish hotspots and maintain uniform temperatures (Khai, 2021). In addition, flight manufacturers also intend to integrate an ice protection system with this noise abatement tool due to its adverse heat transfer characteristics as well as minimizing environmental noise pollution. However, employing this concept in real flight scenarios is challenging due to the cost constraint in experiment and validation. In this sense, CFD analysis gives the great opportunity of studying the comprehensive factors of integrating the ice protection system with noise abatement technique. Surface temperature distribution, bias flow velocity, uniformity of lip skin temperature, and air velocity and temperature profiles inside bias acoustic liner are the important characteristics that are difficult to measure during real flight conditions. However, these characteristics can be predicted by using CFD. Hence, designing and analyzing these systems using CFD before implementation is essential. Furthermore, this system would be designed by extending the noise abatement tool from the nacelle nose cowl zone to the nacelle lip skin. Then, the hot air would be sent to the nacelle lip skin via the PTAI system. Hence, this would be the most effective technique for absorbing excessive engine noise and preventing noise pollution.

## CONCLUSION

The article has reviewed the recent findings regarding integrating ice protection and noise abatement systems. This review emphasizes various factors pertaining to integrating the ice protection system with the noise abatement system. In the present review, various ice protection systems are discussed in detail. Also discussed are the advantages and disadvantages of each ice protection system. Anti-icing studies utilizing CFD have been the subject of a limited number of studies. These are explained properly; the information is very important for future research. In addition, noise abatement tools are crucial, particularly in aircraft, to minimize excessive engine noise that might cause noise pollution to the surroundings; these tools are therefore described in length. As it is essentially important to integrate the ice protection system with the noise abatement system, this

is also explored, along with prior research findings. Thus, this review will be valuable for researchers interested in anti-icing and noise abatement techniques. Recently, many researchers proposed substituting electric motors for jet engines in aircraft thrust systems. The designer of aircraft thermal systems, therefore, faces a new challenge in overcoming icing and noise problems.

## ACKNOWLEDGMENT

The authors acknowledge funding of Universiti Sains Malaysia, Organization for Women in Science for the Developing World (OWSD), and the Swedish International Development Cooperation Agency (SIDA).

## REFERENCES

- Al-Khalil, K., Ferguson, T., & Phillips, D. (1997). A hybrid anti-icing ice protection system. In *35th Aerospace Sciences Meeting and Exhibit* (p. 302). American Institute of Aeronautics and Astronautics. <https://doi.org/10.2514/6.1997-302>
- Al-Khalil, K. (2007, January). Thermo-mechanical expulsive deicing system-TMEDS. In *45th AIAA Aerospace Sciences Meeting and Exhibit* (p. 692). American Institute of Aeronautics and Astronautics. <https://doi.org/10.2514/6.2007-692>
- Asante, C. J., Pokhrel, M., & Cho, J. (2016). CFD simulation study of de-icing on a pitot tube. *International Journal of Applied Engineering Research*, *11*(5), 2986-2989.
- Azam, Q., Ismail, M. A., Mazlan, N. M., & Bashir, M. (2016). Numerical comparison of drag coefficient between nacelle lip-skin with and without bias acoustic liner. *International Review of Mechanical Engineering*, *10*(6), 390-394. <https://doi.org/10.15866/ireme.v10i6.9427>
- Azam, Q., & Ismail, M. A. (2017, August 2). Noise abatement system in commercial aircraft by using Bias Acoustic Liner on nacelle lip-skin. In *International Conference on Vibration, Sound and System Dynamics (ICVSSD)* (p. 49-54). Universiti Sains Malaysia. <https://www.researchgate.net/publication/320584447>
- Azam, Q., & Ismail, M. A. (2018). Experimental study of bias acoustic liner on nacelle lip-skin. *Journal of Mechanical Engineering*, *5*(2), 67-77.
- Barzanouni, Y., Gorji-Bandpy, M., & Tabrizi, H. B. (2020). Simulation of different shapes and arrangements of holes over the leading edge of airfoil by blowing to prevent ice accretion. *Journal of the Brazilian Society of Mechanical Sciences and Engineering*, *42*(9), Article 448. <https://doi.org/10.1007/s40430-020-02524-x>
- Battisti, L. (2015). *Wind turbines in cold climates: Icing impacts and mitigation systems*. Springer.
- Bennani, L., Trontin, P., & Radenac, E. (2023). Numerical simulation of an electrothermal ice protection system in anti-icing and deicing mode. *Aerospace*, *10*(1), Article 75. <https://doi.org/10.3390/aerospace10010075>
- Birbragher, F. (1988). *Nacelle anti-icing system* (U.S. Patent No. 4,738,416). U.S. Patent and Trademark Office. <https://image-ppubs.uspto.gov/dirsearch-public/print/downloadPdf/4738416>

- Bu, X., Lin, G., Yu, J., Yang, S., & Song, X. (2012). Numerical simulation of an airfoil electrothermal anti-icing system. *Proceedings of the Institution of Mechanical Engineers, Part G: Journal of Aerospace Engineering*, 227(10), 1608-1622. <https://doi.org/10.1177/0954410012463525>
- Bu, X., Lin, G., Yu, J., Shen, X., & Hou, P. (2013). Numerical analysis of a swept wing hot air ice protection system. *Proceedings of the Institution of Mechanical Engineers, Part G: Journal of Aerospace Engineering*, 228(9), 1507-1518. <https://doi.org/10.1177/0954410013494515>
- Bu, X., Lin, G., Shen, X., Hu, Z., & Wen, D. (2020). Numerical simulation of aircraft thermal anti-icing system based on a tight-coupling method. *International Journal of Heat and Mass Transfer*, 148, Article 119061. <https://doi.org/10.1016/j.ijheatmasstransfer.2019.119061>
- Cao, Y., Huang, J., & Yin, J. (2016). Numerical simulation of three-dimensional ice accretion on an aircraft wing. *International Journal of Heat and Mass Transfer*, 92, 34-54. <https://doi.org/10.1016/j.ijheatmasstransfer.2015.08.027>
- Cao, Y., Tan, W., Su, Y., Xu, Z., & Zhong, G. (2020). The effects of icing on aircraft longitudinal aerodynamic characteristics. *Mathematics*, 8(7), Article 1171. <https://doi.org/10.3390/math8071171>
- Croce, G., Habashi, W. G., Guevremont, G., & Tezok, F. (1998). *3D thermal analysis of an anti-icing device using FENSAP-ICE*. In *36th AIAA Aerospace Sciences Meeting and Exhibit* (p. 193). American Institute of Aeronautics and Astronautics. <https://doi.org/10.2514/6.1998-193>
- de Mattos, B. S., & Oliveira, G. L. (2000). Three-dimensional thermal coupled analysis of a wing slice slat with a piccolo tube. In *18th Applied Aerodynamics Conference* (p. 3921). American Institute of Aeronautics and Astronautics. <https://doi.org/10.2514/6.2000-3921>
- Domingos, R. H., Papadakis, M., & Zamora, A. O. (2010). *Computational methodology for bleed air ice protection system parametric analysis*. In *AIAA Atmospheric and Space Environments Conference* (p. 7834). American Institute of Aeronautics and Astronautics. <https://doi.org/10.2514/6.2010-7834>
- Elangovan, R., & Hung, K. E. (2007). Minimum heating energy requirements of piccolo tube jet impingement thermal anti-icing system. In *ASME/JSME 2007 Thermal Engineering Heat Transfer Summer Conference (Vol. 1, pp. 959-967)*. The American Society of Mechanical Engineers. <https://doi.org/10.1115/ht2007-32080>
- Goraj, Z. (2004). *An overview of the de-icing and anti-icing technologies with prospects for the future*. In *24th International Congress of the Aeronautical Sciences* (Vol. 29). International Council of the Aeronautical Sciences.
- Grishaev, V. G., Borodulin, I. S., Usachev, I. A., Amirfazli, A., Drachev, V. P., Rudenko, N. I., Gattarov, R. K., Bakulin, I. K., Makarov, M. V., & Akhatov, I. S. (2021). Anti-icing fluids interaction with surfaces: Ice protection and wettability change. *International Communications in Heat and Mass Transfer*, 129, Article 105698. <https://doi.org/10.1016/j.icheatmasstransfer.2021.105698>
- Hannat, R., & Morency, F. (2014). Numerical validation of conjugate heat transfer method for anti-/de-icing piccolo system. *Journal of Aircraft*, 51(1), 104-116. <https://doi.org/10.2514/1.c032078>
- Hassaani, A., Elsayed, A. F., & Khalil, E. E. (2020). Numerical investigation of thermal anti-icing system of aircraft wing. *International Robotics & Automation Journal*, 6(2), 60-65. <https://doi.org/10.15406/iratj.2020.06.00202>

- Huanyu, D., Chang, S., & Mengjie, S. (2020). The optimization of simulated icing environment by adjusting the arrangement of nozzles in an atomization equipment for the anti-icing and deicing of aircrafts. *International Journal of Heat and Mass Transfer*, 155, Article 119720. <https://doi.org/10.1016/j.ijheatmasstransfer.2020.119720>
- Hoffman, D. A. (2007). *Experimental investigation of turbojet thrust augmentation using an ejector* [Doctoral dissertation]. Air Force Institute of Technology, USA. <https://scholar.afit.edu/cgi/viewcontent.cgi?article=3966&context=etd>
- Hua, J., Kong, F., & Liu, H. H. T. (2007). Unsteady thermodynamic computational fluid dynamics simulations of aircraft wing anti-icing operation. *Journal of Aircraft*, 44(4), 1113-1117. <https://doi.org/10.2514/1.24122>
- Hua, J., & Liu, H. H. (2005). Fluid flow and thermodynamic analysis of a wing anti-icing system. *Canadian Aeronautics and Space Journal*, 51(1), 35-40. <https://doi.org/10.5589/q05-004>
- Ismail, M. A. (2013). *Enhancement of heat transfer performance on nacelle lip-skin for swirl anti-icing* [Unpublished Doctoral dissertation]. Kingston University, England.
- Ismail, M. A., & Abdullah, M. Z. (2015). Applying computational fluid dynamic to predict the thermal performance of the nacelle anti-icing system in real flight scenarios. *Indian Journal of Science and Technology*, 8(30), Article 66. <https://doi.org/10.17485/ijst/2015/v8i30/86058>
- Ismail, M. A., & Wang, J. (2018). Effect of nozzle rotation angles and sizes on thermal characteristic of swirl anti-icing. *Journal of Mechanical Science and Technology*, 32(9), 4485-4493. <https://doi.org/10.1007/s12206-018-0845-x>
- Ives, A. O. (2009). *Perforated honeycomb acoustic liner heat transfer* [Unpublished Doctoral dissertation]. Queen University Belfast, UK.
- Ives, A. O., Wang, J., Raghunathan, S., & Sloan, P. (2011). Heat transfer through single hole bias flow acoustic liner. *Journal of Thermophysics and Heat Transfer*, 25(3), 409-423. <https://doi.org/10.2514/1.T3637>
- Jiang, X., & Wang, Y. (2019). Studies on the electro-impulse de-icing system of aircraft. *Aerospace*, 6(6), Article 67. <https://doi.org/10.3390/aerospace6060067>
- Jun, S., Dongguang, X., Lin, Y., & Dongyu, Z. (2020). *Experimental study of hybrid deicing system*. *IOP Conference Series: Materials Science and Engineering*, 751, Article 012042. <https://doi.org/10.1088/1757-899X/751/1/012042>
- Khai, L. C. (2021). *CFD study on thermal characteristics of acoustic liner and bias acoustic liner in real flight conditions* [Unpublished Master's thesis]. University Sains Malaysia, Malaysia.
- Khai, L. C., Ismail, M. A., Azam, Q., & Mazlan, N. M. (2020). Experimental study on aerodynamic performance of nacelle lip-skin bias flow. *Journal of Mechanical Science and Technology*, 34(4), 1613-1621. <https://doi.org/10.1007/s12206-020-0323-0>
- Khalil, E. E., Said, E., AlSaleh, A., & ElHariry, G. (2020). *Effect of hot air jet arrangement from a piccolo tube in aircraft wing anti-icing system*. In *AIAA Propulsion and Energy 2020 Forum* (p. 3952). American Institute of Aeronautics and Astronautics. <https://doi.org/10.2514/6.2020-3952>
- Liu, Q., Yang, Y., Wang, Q., Cui, Y., & Cai, J. (2019). Icing performance of stratospheric airship in ascending process. *Advances in Space Research*, 64(11), 2405-2416. <https://doi.org/10.1016/j.asr.2019.09.013>

- Ma, Q. (2011). *Aircraft icing and thermo-mechanical expulsion de-icing technology* [Master's thesis]. Cranfield University, UK. [https://dspace.lib.cranfield.ac.uk/bitstream/handle/1826/12478/Ma\\_Q\\_2010.pdf?sequence=1&isAllowed=y](https://dspace.lib.cranfield.ac.uk/bitstream/handle/1826/12478/Ma_Q_2010.pdf?sequence=1&isAllowed=y)
- Moe, J. W., Wunsch, J. J., & Sperling, M. S. (2009). *Method and apparatus for noise abatement and ice protection of an aircraft engine nacelle inlet lip*. (U.S. Patent No. 7,588,212). U.S. Patent and Trademark Office. <https://image-ppubs.uspto.gov/dirsearch-public/print/downloadPdf/7588212>
- Morency, F., Brahimi, M., Tezok, F., & Paraschivoiu, I. (1997). Hot air anti-icing system modelization in the ice prediction code CANICE. In *36th AIAA Aerospace Sciences Meeting and Exhibit* (p. 192). American Institute of Aeronautics and Astronautics. <https://doi.org/10.2514/6.1998-192>
- Morency, F., Tezok, F., & Paraschivoiu, I. (2000). Heat and mass transfer in the case of anti-icing system simulation. *Journal of Aircraft*, 37(2), 245-252. <https://doi.org/10.2514/2.2613>
- Nagappan, N. M. (2013). *Numerical modeling of anti-icing using an array of heated synthetic jets* [Doctoral dissertation]. Embry-Riddle Aeronautical University, Florida. <https://commons.erau.edu/cgi/viewcontent.cgi?article=1108&context=edt>
- Papadakis, M., & Wong, S. H. J. (2006). Parametric investigation of a bleed air ice protection system. In *44th AIAA Aerospace Sciences Meeting and Exhibit* (p. 1013). American Institute of Aeronautics and Astronautics. <https://doi.org/10.2514/6.2006-1013>
- Petrenko, V. F. (2005). *System and method for modifying ice-to-object interface* (U.S. Patent No. 6,870,139). U.S. Patent and Trademark Office. <https://image-ppubs.uspto.gov/dirsearch-public/print/downloadPdf/6870139>
- Raghunathan, S., Benard, E., Watterson, J. K., Cooper, R. K., Curran, R., Price, M., Yao, H., Devine, R., Crawford, B., Riordan, D., Linton, A., Richardson, J., & Tweedie, J. (2006). Key aerodynamic technologies for aircraft engine nacelles. *The Aeronautical Journal*, 110(1107), 265-288. <https://doi.org/10.1017/s0001924000013154>
- Ramamurthy, S., Keith, T. G., Jr., De Witt, K. J., Putt, J. C., Martin, C. A., & Leffel, K. L., (1991). Numerical modelling of an advanced pneumatic impulse ice protection system (PIIP) for aircraft. In *AIAA 29th Aerospace and Science Meeting* (p. 555). American Institute of Aeronautics and Astronautics. <https://doi.org/10.2514/6.1991-555>
- Reid, T., Baruzzi, G. S., & Habashi, W. G. (2012). FENSAP-ICE: Unsteady conjugate heat transfer simulation of electrothermal de-icing. *Journal of Aircraft*, 49(4), 1101-1109. <https://doi.org/10.2514/1.c031607>
- Rigby, D. (2006). *Numerical investigation of hole pattern effect on piccolo tube anti-icing*. In *44th AIAA Aerospace Sciences Meeting and Exhibit* (p. 1012). American Institute of Aeronautics and Astronautics. <https://doi.org/10.2514/6.2006-1012>
- Rohini, D., Lokesgarun, D., Naveen, R., & Samiyappan, P. (2019). Comparison of rotating piccolo tube with fixed piccolo tube by using CFD. *International Journal of Engineering and Technology*, 11(1), 26-34. <https://doi.org/10.21817/ijet/2019/v11i1/191101017>
- Ronauo, R. J., Batterson, J. G., Reehors, A. L., Bonds, T. H., & O'Mara, T. M. (1991). Effect of tail ice on longitudinal aerodynamic derivatives. *Journal of Aircraft*, 28(3), 193-199. <https://doi.org/10.2514/3.46012>

- Rosenthal, H. A., & Nelepovitz, D. O. (1985). *AIAA/SAE/ASME/ASEE 21st Joint Propulsion Conference, Monterey California*. American Institute of Aeronautics and Astronautics
- Shen, X., Lin, G., Yu, J., Bu, X., & Du, C. (2013). Three-dimensional numerical simulation of ice accretion at the engine inlet. *Journal of Aircraft*, 50(2), 635-642. <https://doi.org/10.2514/1.c031992>
- Smith, A. G., & Taylor, K. (1997). The simulation of an aircraft engine intake anti-icing system. *The PHOENICS Journal of Computational Fluid Dynamics and its Applications*, 10(2), 150-166.
- Sreedharan, C., Nagpurwala, Q. H., Subbaramu, S. (2014). Effect of hot air jets from a piccolo tube in aircraft wing anti-icing unit. *SASTech - Technical Journal of RUAS*, 13(2), 2-5.
- Syed, M. H. Y., Ismail, M. A., Azam, Q., Rajendran, P., & Mazlan, N. M. (2018). Simulation study of the effect of anti-icing on the nacelle lip-skin material. In *IOP Conf. Series: Materials Science and Engineering* (Vol. 370, p. 012011). IOP Publishing. <https://doi.org/10.1088/1757-899X/370/1/012011>
- United States National Transportation Safety Board. (2007). *Aircraft accident report: Crash during approach to landing, circuit city stores, Inc., Cessna citation 560, N500AT, Pueblo, Colorado, February 16, 2005*. [https://reports.aviation-safety.net/2007/20070317-1\\_C500\\_N511AT.pdf](https://reports.aviation-safety.net/2007/20070317-1_C500_N511AT.pdf)
- Wang, H., Tran, P., Habashi, W. G., Chen, Y., Zhang, M., & Feng, L. (2007). *Anti-icing simulation in wet air of a piccolo system using FENSAP-ICE*. SAE Technical Paper 2007-01-3357. SAE International. <https://doi.org/10.4271/2007-01-3357>
- Wang, Z., Zhao, H., & Liu, S. (2022). Numerical Simulation of Aircraft Icing under Local Thermal Protection State. *MDPI Aerospace*, 9(2), Article 84. <https://doi.org/10.3390/aerospace9020084>
- Wong, S. H., Papadakis, M., & Zamora, A. (2009). *Computational Investigation of Bleed Air Ice Protection System*. In *1st AIAA Atmospheric and Space Environments Conference* (p. 3966). American Institute of Aeronautics and Astronautics. <https://doi.org/10.2514/6.2009-3966>
- Yang, K., Liu, Q., Lin, Z., Liang, Y., & Liu, C. (2022). Investigations of interfacial heat transfer and droplet nucleation on bioinspired superhydrophobic surface for anti-icing/de-icing. *SSRN Electronic Journal*, 1-22. <https://doi.org/10.2139/ssrn.4002238>
- Zhou, Y., Lin, G., Bu, X., Mu, Z., Pan, R., Ge, Q., & Qiao, X. (2017, March). Temperature and Runback Ice Prediction Method for Three-Dimensional Hot Air Anti-Icing System. In *IOP Conference Series: Materials Science and Engineering* (Vol. 187, No. 1, p. 012017). IOP Publishing. <https://doi.org/10.1088/1757-899x/187/1/012017>
- Zheng, M., Guo, Z., Dong, W., & Guo, X. (2019). Experimental investigation on ice accretion on a rotating aero-engine spinner with hydrophobic coating. *International Journal of Heat and Mass Transfer*, 136, 404-414. <https://doi.org/10.1016/j.ijheatmasstransfer.2019.02.104>

